stabilities on the DME and H_2O complexes.

On the other hand, a comparison of the ER and AIC regarding the relative stabilities of the TMA and DMA complexes is more consistent. The results for d(S···N), ϵ, and ΔE_{diss} indicate that TMA·SO_2 is slightly more stable than DMA·SO_2, probably by about 0.5-1.0 kcal/mol (the STO-3G calculation is again an exception). The stabilizing effect from methyl substitution in amines has been discussed extensively in the literature and was summarized recently.[6] The Morokuma energy analysis indicates that increases in both the polarization and charge-transfer terms parallel the overall increase in stability with methyl substitution. While the evidence is not as compelling in the case of the ether/water complexes, it appears (from the experimental d(S···O) and ϵ) that the water complex may be slightly more stable than the ether complex. It was pointed out above (see structure and dipole sections) that competing effects occur here: the dipole moments of water (1.85 D) and DME (1.30 D) favor H_2O·SO_2, while the increased polarizability of DME from methyl substitution (DME·SO_2, $\mu_{induced}$ = 1.41 D; H_2O·SO_2, $\mu_{induced}$ = 0.75 D) favors DME·SO_2. This makes it difficult to qualitatively predict the more stable dimer. It is interesting that the difference in proton affinities favors DME by 22 kcal/mol over H_2O,[15a] which is not reflected in the experimental structures of their SO_2 complexes or in their stabilities, which appear roughly equal. In contrast, the difference in proton affinities for TMA and DMA of 4.2 kcal/mol[15a] favors TMA and is closer to the estimated differences in their binding energies (~1 kcal/mol) and the change in d(N···S) in their SO_2 complexes.

The ER and AIC concur that a methyl group staggers the SO_2 group in the amine complexes, while methyl groups eclipse the S-O bonds in DME·SO_2. One factor is the antiparallel orientation of the monomer dipoles in DME·SO_2, which will maximize the electrostatic interaction at the expense of the eclipsing arrangement. In the amine·SO_2 complexes, the dipole moments of the monomers are nearly perpendicular and eclipsing of the O-Me and S-O bonds is no longer a geometric consequence. Also, the short N···S and longer O···S interaction distances in the two types of complexes provide different interaction regimes; obviously, repulsive interactions between eclipsed groups may be more important in the amine complexes.

In summary, while the ER and AIC agree on many of the geometric and energetic trends, it is apparent that the AIC provide mixed results in terms of the energetics and structural parameters. The problem in calculating ΔE_{diss} is a well-known one, endemic to the problem of estimating a small number from the difference between two large numbers.[41] The neglect of correlation effects and basis set superposition corrections as well as the limited basis sets are the root of this difficulty. The observation that the gross geometries can be reasonably approximated by these HF-level calculations is gratifying. Nevertheless, regarding detailed geometries, the STO-3G calculations do reasonably well for d(S···O) in the ether/water complexes but poorly for the amine complexes, while the opposite is true for calculations at a higher level (such as 3-21G), which makes it difficult to propose any working hypothesis about choosing basis sets for new systems. More comparisons between theory and experiment for a broader set of complexes may serve to establish better guidelines for the reliability of such HF-level structural parameters for systems as complicated as these.

Acknowledgment. We are grateful to the donors of the Petroleum Research Fund, administered by the American Chemical Society, for support of this work. The research was also supported by the National Science Foundation.

Registry No. $(CH_3)_2O$·SO_2, 42383-26-6; ^{34}S, 13965-97-4; ^{18}O, 14797-71-8; ^{13}C, 14762-74-4.

(41) A discussion of this difficulty was recently given: Hess, O.; Caffarel, M.; Huiszoon, C.; Claverie, P. *J. Chem. Phys.* **1990**, *92*, 6049.

Contribution from the Department of Chemistry and Chemical Physics Program, Washington State University, Pullman, Washington 99164-4630

Structural Dependence of the Luminescence from Bis(substituted benzenethiolato)(2,9-dimethyl-1,10-phenanthroline)zinc(II) Complexes

K. J. Jordan, W. F. Wacholtz, and G. A. Crosby*

Received August 22, 1989

Changes in luminescence spectra and lifetimes of crystalline samples of the title compounds at 77 K are correlated with phase changes of the solids. The ease of conversion among phases is a general property of this class of materials. For bis(benzenethiolato)(2,9-dimethyl-1,10-phenanthroline)zinc(II) complete structure determinations were made of both phases. The attendant changes of the optical properties are ascribed to rotation of the planes of the two thiol rings on a single zinc ion from an approximately perpendicular to a nearly face-to-face conformation as the slowly heated crystal undergoes the phase change. The relevance of these results to the problem of charge separation in solids is discussed.

Introduction

Luminescence from zinc complexes has been used extensively in this laboratory to monitor the effects of subtle structural changes upon the relative rates of radiative and radiationless processes in the crystals and solids. Of particular interest is the process of charge separation after optical excitation. Recently we extended our studies to the solid state where thermal barriers to radiationless processes have been observed.[1] In the course of these investigations, we have discovered that some of the complexes exhibit at least two crystalline phases and that the attendant luminescence properties are sensitive functions of the phase purity. Moreover, complete conversion to the high-temperature phase can be accomplished by heating to temperatures just below the melting point. Preliminary data on several complexes are described, and a detailed crystallographic study of two phases of the Zn(PhS)$_2$(2,9-Me$_2$phen) complex is reported.[2] For this latter system, the principal structural difference of the phases involves the relative orientation of the phenyl rings of the two coordinated thiols.

Experimental Section

Synthesis. To a solution of zinc acetate dihydrate (0.22 g, 1 mmol) dissolved in 100 mL of hot ethanol a solution of redistilled benzenethiol (0.21 mL, 2.1 mmol in 10 mL of ethanol) was added dropwise with stirring. As the second millimole was added, a white precipitate formed. After 5 min of continual stirring, 2,9-dimethyl-1,10-phenanthroline (0.21

(1) Highland, R. G.; Crosby, G. A. *Chem. Phys. Lett.* **1985**, *119*, 454.

(2) Compounds are identified in Table V.

0020-1669/91/1330-4588$02.50/0

Table I. Crystallographic Data for the Monoclinic and Orthorhombic Crystals of $Zn(PhS)_2(2,9\text{-}Me_2phen)$

	monoclinic	orthorhombic
chem formula	$ZnC_{26}H_{22}N_2S_2$	$ZnC_{26}H_{22}N_2S_2$
fw	491.69	491.69
space group	$C2/c$	$Pbca$
a, Å	15.418 (3)	27.296 (8)
b, Å	13.154 (2)	13.941 (3)
c, Å	11.556 (2)	12.139 (5)
β, deg	101.46 (1)	
V, Å^3	2297.1 (6)	4619 (2)
Z	4	8
T	ambient	ambient
λ, Å	0.71069	0.71069
ρ_{calcd}, g cm^{-3}	1.42	1.41
μ, cm^{-1}	12.9	12.8
$R(F_o)$	0.0539	0.0864
$R_w(F_o)$	0.0493	0.0490

g, 1 mmol) dissolved in 10 mL of ethanol was added dropwise. The mixture was heated and stirred for $^1/_2$ h as it gradually turned to a deep yellow solution. It was set aside to cool. After 2–3 days at room temperature, crystals were harvested and washed with ethanol. Although the reactions were routinely carried out under N_2, the products did not appear to be air-sensitive. A faint odor of thiol was evident when sample vials were opened, but old samples produced luminescence essentially indistinguishable from fresh ones. All the compounds reported in this article were synthesized by the same method.

Although $Zn(PhS)_2(2,9\text{-}Me_2phen)$ generally produced monoclinic crystals, recrystallization of a sample at room temperature in an open beaker yielded, adventitiously, a crop of large orthorhombic needles. We have been unable to repeat this result, but enough orthorhombic crystals were acquired to carry out the series of measurements reported here on that phase. In the case of $Zn(4\text{-}ClPhS)_2(2,9\text{-}Me_2phen)$ two crystal types were obtained simultaneously from the mother liquor and could be separated mechanically. The $Zn(PhS)_2(2,9\text{-}Me_2\text{-}4,7\text{-}Ph_2phen)$ molecule was only obtained in the low-temperature phase during the initial crystallization process.

Optical Measurements. Emission studies at 77 K were performed in a Pyrex Dewar. Crystals were suspended in a thin film of mineral oil that was held by surface tension within a wire loop immersed in liquid N_2. The samples were excited by the 364-nm line from a Coherent 90-5 UV argon ion laser. Typical intensities were 0.3 mW mm^{-2}. The emitted light was dispersed by an Instruments SA HR-640 grating monochromator (1200 lines/mm) and detected with a Hammamatsu R943 photomultiplier. The signal was measured by a Stanford Research Systems SR400 photon counter in either CW or gated mode. All reported spectra were corrected for spectral response of the system by means of a standard tungsten lamp.

For lifetime measurements the CW beam was square-wave-modulated with a Conoptics Model 10/380 Electro-optic Modulator driven by a Wavetek 191 Function Generator. The time resolution (100 ns) was limited by the 10-MHz response frequency of the modulator. The curves were fit over 5 decay times for which the baseline was chosen to be at the minimum point. This procedure was necessary because the system does not provide 100% depth of modulation.

DSC Measurements. The differential scanning calorimetric measurement was performed on a Perkin-Elmer DSC7 instrument. Orthorhombic $Zn(PhS)_2(2,9\text{-}Me_2phen)$ crystals (14.3 mg) were ground to a fine powder and sealed in an aluminum sample cup. The reference was a similar can sealed with air. A scan rate of 10 °C/min was employed. A 77 K emission spectrum confirmed that grinding the crystals did not induce a phase change.

Crystallographic Data Collection and Structure Determinations. X-ray diffraction data collections were performed on a Syntex $P2_1$ diffractometer upgraded to Nicolet P3F specifications, and the structures were solved by employing direct methods with version 5.1 of the SHELXTL structure solution package.[3] Data for both forms of $Zn(PhS)_2(2,9\text{-}Me_2phen)$ were collected by means of graphite monochromated Mo Kα radiation.[4] Accurate unit cell parameters were obtained through centering of 25 reflections with 2θ values between 29 and 36° for the monoclinic form and 2θ and 26° for the orthorhombic form of the complex. For empirical absorption corrections an ellipsoidal crystal for both the monoclinic and orthorhombic forms of the complex was assumed.

(3) Sheldrick, G. *SHELXTL*; Nicolet Analytical Instruments: Madison, WI, 1985.

(4) Campana, C. F.; Shepard, D. F.; Litchman, W. M. *Inorg. Chem.* **1981**, *20*, 4039.

Table II. Selected Interatomic Distances (Å) for the Monoclinic and Orthorhombic Forms of $Zn(PhS)_2(2,9\text{-}Me_2phen)$

	monoclinic	orthorhombic
Zn–S(1)	2.255 (2)	2.257 (4)
Zn–S(2)	2.255 (2)	2.270 (3)
Zn–N(1)	2.086 (4)	2.128 (7)
Zn–N(2)	2.086 (4)	2.114 (7)
S(1)–C(1)	1.758 (4)	1.768 (10)
S(2)–C(7)	1.758 (4)	1.777 (9)
C(1)–C(2)	1.391 (7)	1.362 (15)
C(1)–C(6)	1.388 (7)	1.398 (15)
C(7)–C(8)	1.391 (7)	1.395 (14)
C(7)–C(12)	1.388 (7)	1.381 (14)

Table III. Selected Interatomic Angles (deg) for the Monoclinic and Orthorhombic Forms of $Zn(PhS)_2(2,9\text{-}Me_2phen)$

	monoclinic	orthorhombic
S(1)–Zn–S(2)	134.5 (1)	138.1 (1)
S(1)–Zn–N(1)	106.7 (1)	106.2 (2)
S(2)–Zn–N(1)	107.7 (1)	103.9 (2)
S(1)–Zn–N(2)	107.7 (1)	105.3 (2)
S(2)–Zn–N(2)	106.7 (1)	108.6 (2)
N(1)–Zn–N(2)	80.2 (2)	79.0 (3)
Zn–S(1)–C(1)	109.8 (2)	110.4 (4)
Zn–S(2)–C(2)	109.8 (2)	111.9 (3)
C(2)–C(1)–S(1)	124.5 (4)	120.6 (8)
C(6)–C(1)–S(1)	117.5 (4)	121.8 (8)
C(8)–C(7)–S(2)	124.5 (4)	117.9 (7)
C(12)–C(7)–S(2)	117.5 (4)	124.3 (7)

Pertinent crystallographic parameters are included in Table I with a more complete table of crystallographic parameters available through supplementary material.

For both forms of $Zn(PhS)_2(2,9\text{-}Me_2phen)$, direct methods revealed the zinc atoms. Subsequent difference maps revealed the positions of all other non-hydrogen atoms. Hydrogen atoms were fixed at calculated positions ($r_{C\text{-}H}$ = 0.96 Å). The thermal parameters were anisotropic on all non-hydrogen atoms for the monoclinic form of the complex. For the orthorhombic form the thermal parameters were anisotropic on all non-carbon, non-hydrogen atoms and on selected carbon atoms expected to exhibit the most thermal motion (Table IV). The thermal parameters for all hydrogen atoms were fixed at approximately 1.2 times the corresponding heavier atom thermal parameter. Selected bond lengths and angles are given in Tables II and III, respectively. Atomic coordinates and thermal parameters are given in Table IV. The standard ACS X-ray data collection parameters long form, complete listings of bond lengths and angles, complete listings of hydrogen atom positions and anisotropic thermal parameters as well as a tabulation of the $|F_o|$ and $|F_c|$ values have been deposited.

Results

Phase Changes. The incidence of a phase transition could be monitored visually in a melting point apparatus. For $Zn(PhS)_2(2,9\text{-}Me_2phen)$, as the temperature of the low-temperature phase (orthorhombic) was raised, a subtle, but definite, cracking could be observed over a narrow range. No other physical changes were evident until the crystals approached their melting points where a decided darkening of the color set in. Once taken through the phase change, by heating, the crystals remained in the high-temperature phase upon cooling. Holding the temperature for several days just below the transition temperature did not regenerate the second phase. The phase transition temperatures as determined by cracking are given in Table V along with the melting points.

A differential scanning calorimetric measurement was performed on a powdered sample of $Zn(PhS)_2(2,9\text{-}Me_2phen)$ in the orthorhombic phase. The onset of an endothermic transition was detected by DSC at 140 °C and finally peaked at 144 °C.

Structure Description. Both forms of the complex $Zn(PhS)_2(2,9\text{-}Me_2phen)$ pack as discrete molecules with a distorted tetrahedral geometry around the central zinc atom (Figure 1). The zinc–sulfur bond lengths are 2.255 (2) Å for $Zn\text{–}S_1$ and $Zn\text{–}S_2$ in the monoclinic form and 2.257 (4) and 2.270 (3) Å in the orthorhombic form, respectively. For a regular tetrahedron, bond angles would be expected to be 109.5°; however, in both forms of the complex the bond angles are notably different from this

Table IV. Atomic Positional Parameters (× 10^4) for the Monoclinic and Orthorhombic Forms of $Zn(PhS)_2(2,9\text{-}Me_2phen)$

	monoclinic				orthorhombic			
	x	*y*	*z*	U^a	*x*	*y*	*z*	U^a
Zn	0	2617 (1)	2500	49 (1)*	1291 (1)	4609 (1)	3496 (1)	44 (1)*
S(1)	1108 (1)	1954 (1)	1725 (1)	77 (1)*	1928 (1)	5162 (2)	4500 (3)	87 (2)*
S(2)[b]					705 (1)	5209 (2)	2364 (3)	61 (1)*
N(1)[b]					1553 (3)	3377 (5)	2646 (7)	39 (3)*
N(2)	−518 (2)	3830 (3)	1417 (3)	55 (1)*	980 (3)	3498 (5)	4453 (6)	36 (3)*
C(1)	1381 (3)	739 (3)	2320 (4)	57 (2)*	1913 (4)	6429 (7)	4566 (9)	45 (3)
C(2)	1034 (3)	308 (4)	3229 (4)	69 (2)*	2110 (4)	6969 (8)	3742 (9)	57 (4)
C(3)	1269 (3)	−667 (4)	3627 (5)	72 (2)*	2125 (4)	7967 (8)	3816 (10)	64 (4)
C(4)	1851 (4)	−1229 (4)	3139 (5)	78 (2)*	1937 (4)	8418 (8)	4710 (10)	64 (4)
C(5)	2208 (4)	−808 (4)	2251 (5)	80 (2)*	1741 (4)	7903 (7)	5551 (9)	61 (4)
C(6)	1971 (3)	165 (4)	1829 (4)	65 (2)*	1733 (4)	6903 (7)	5497 (10)	61 (4)
C(7)[b]					633 (3)	6468 (6)	2531 (8)	31 (3)
C(8)[b]					391 (3)	6973 (7)	1700 (9)	53 (3)
C(9)[b]					317 (4)	7948 (8)	1823 (9)	61 (4)
C(10)[b]					477 (3)	8433 (7)	2734 (9)	55 (3)
C(11)[b]					706 (3)	7944 (7)	3581 (9)	57 (3)
C(12)[b]					781 (3)	6973 (7)	3451 (9)	50 (3)
C(13)[b]					1841 (4)	3340 (7)	1751 (10)	52 (3)
C(14)[b]					1970 (3)	2448 (8)	1307 (8)	58 (3)
C(15)[b]					1823 (3)	1633 (7)	1774 (8)	51 (4)*
C(16)[b]					1522 (3)	1633 (7)	2709 (8)	43 (3)
C(17)[b]					1353 (4)	782 (7)	3249 (9)	62 (5)*
C(18)	−266 (6)	6589 (4)	1998 (11)	154 (9)*	1059 (4)	876 (8)	4154 (10)	68 (6)*
C(19)	−553 (5)	5676 (4)	1379 (8)	102 (3)*	920 (4)	1766 (7)	4626 (9)	48 (3)
C(20)	−1095 (6)	5603 (7)	273 (10)	136 (5)*	634 (3)	1894 (7)	5555 (8)	58 (5)*
C(21)	−1350 (5)	4682 (8)	−231 (7)	123 (4)*	526 (4)	2789 (8)	5918 (9)	57 (4)
C(22)	−1053 (4)	3785 (5)	352 (5)	80 (3)*	699 (4)	3585 (7)	5338 (8)	42 (3)
C(23)	−284 (3)	4738 (3)	1923 (4)	66 (2)*	1092 (3)	2605 (8)	4079 (8)	35 (3)
C(24)[b]					1396 (3)	2539 (6)	3121 (7)	32 (3)
C(25)[b]					1999 (4)	4277 (8)	1305 (10)	78 (6)*
C(26)	−1277 (4)	2777 (5)	−148 (5)	113 (3)*	584 (4)	4587 (8)	5736 (8)	67 (5)*

[a] Isotropic thermal parameters (Å² × 10^3) with values for anisotropic atoms marked with an asterisk. Equivalent isotropic *U* is defined as one-third of the trace of the orthogonalized U_{ij} tensor. [b] Atoms generated by an inversion symmetry operation.

Table V. Phase Change Temperatures, Melting Points, and Decay Times

compound[a]	phase change, °C[b]	mp, °C	τ(77 K),[c] μs
$Zn(PhS)_2(2,9\text{-}Me_2phen)$			
monoclinic	...	217–218	230[d,e]
orthorhombic	136–143	217–218	<0.1, 0.3, 1.3[d]
$Zn(4\text{-}ClPhS)_2(2,9\text{-}Me_2phen)$			
translucent yellow crystals	...	224–225	5[d,e]
clear yellow crystals	185–187	224–225	3.9, 28[d]
$Zn(PhS)_2(2,9\text{-}Me_2\text{-}4,7\text{-}Ph_2phen)$			
high-temperature phase		181–183	15, >1000[f]
low-temperature phase	125–130	181–183	7, 99[f]
$Zn(F_5PhS)_2(2,9\text{-}Me_2phen)$	180–182	206–207	

[a] $Zn(PhS)_2(2,9\text{-}Me_2phen)$ = bis(benzenethiolato)(2,9-dimethyl-1,10-phenanthroline)zinc(II); $Zn(4\text{-}ClPhS)_2(2,9\text{-}Me_2phen)$ = bis(4-chlorobenzenethiolato)(2,9-dimethyl-1,10-phenanthroline)zinc(II); $Zn(PhS)_2(2,9\text{-}Me_2\text{-}4,7\text{-}Ph_2phen)$ = bis(benzenethiolato)(2,9-dimethyl-4,7-diphenyl-1,10-phenanthroline)zinc(II); $Zn(F_5PhS)_2(2,9\text{-}Me_2phen)$ = bis(pentafluorobenzenethiolato)(2,9-dimethyl-1,10-phenanthroline)-zinc(II). [b] Estimated from observing cracking in melting point apparatus. [c] λ_{ex} = 363.8 nm. [d] Measured at 600 nm. [e] Exponential decay. [f] Measured at 650 nm, dominant components.

ideal value (Table III). This is expected due to the nature of the N,N-heterocycle and the possibility of a large degree of flexibility of the thiol ligand. The $2,9\text{-}Me_2phen$ ligand defines a plane in both forms of the complex and exhibits a rocking motion in that plane as observed from the thermal ellipsoids shown in Figure 1. It appears that the methyl substituents effectively lock in the ligand so that motion perpendicular to the plane of the ligand is significantly reduced when compared to other planar N,N-heterocyclic ligands that lack methyl substituents.

Depending on the crystal form, the benzenethiolate ligands adopt a different orientation with respect to each other. In the monoclinic phase, they are more face to face and are in fact

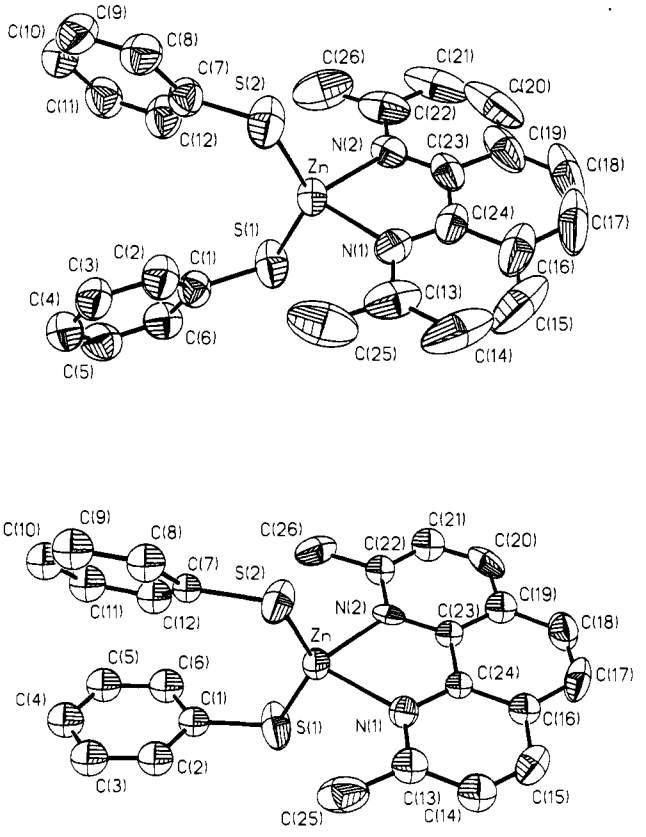

Figure 1. Thermal ellipsoid plots of the structure of $Zn(PhS)_2(2,9\text{-}Me_2phen)$: (top) monoclinic phase; (bottom) orthorhombic phase.

symmetrically related through a molecular C_2 rotation. In the orthorhombic form, the planes of the benzene rings are more perpendicular to each other and are not related by symmetry. This

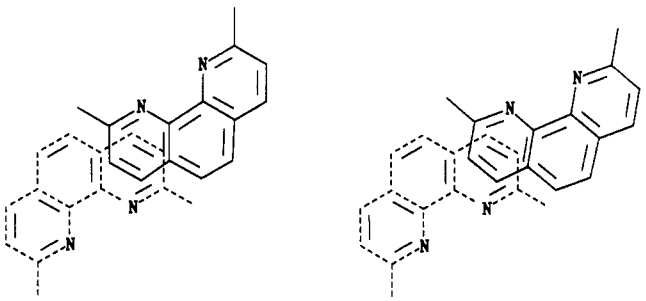

Figure 2. Projection diagrams of $Zn(PhS)_2(2,9\text{-}Me_2phen)$ showing overlaps of N,N-heterocyclic rings of adjacent molecules.

understandably affects the bond angles around the sulfur atoms in these two complexes (Table III) and might account for the observed photophysical differences (vide infra). There appear to be no abnormally long carbon–nitrogen, carbon–carbon, or carbon–sulfur bonds in either of the two crystalline forms.

The planes of one substituted-phenanthroline ligand overlap with a substituted-phenanthroline ligand on an adjacent molecule to produce a pseudodimer (Figure 2). The overlap, however, is not substantial and has been observed to be more extensive in crystals of other multinuclear zinc dithiol complexes.[5] The distances separating the two ligands within the pseudodimer are 3.36 (1) and 3.45 (1) Å for the monoclinic and orthorhombic forms, respectively. Both phases of the complex appear to exhibit their pseudodimeric packing with benzenethiol ligands located between the pseudodimers (Figure 3); however, there is no significant overlap of the thiol ligands with the phenanthroline moieties of the pseudodimer units. We note that this packing does not appear to generate a one-dimensional linear chain system in either form, since only interactions within the pseudodimers are possible.

Spectral Data. Essential emission spectra are presented in Figures 4–6. In Figure 4 the spectrum of the orthorhombic phase of $Zn(PhS)_2(2,9\text{-}Me_2phen)$ is seen to peak at 660 nm, whereas that of the monoclinic phase maximizes at 565 nm. Although the plotted spectra are normalized, the latter emission is significantly (5×) brighter than the former. Moreover, a hint of structure appears on the high-energy side of the spectrum of the monoclinic crystals. This feature is enhanced when the sample is cooled to 4.5 K (not shown) but never appears in the emission from the orthorhombic material. (There is also a very weak long-lived structured $\pi\pi^*$ phosphorescence in the 77 K spectrum of the monoclinic phase that is highly self-absorbed by the crystal in the 440–470-nm range. Its similarity to that of the free ligand clearly identifies it as $^3\pi\pi^*$ emission from the 2,9-Me_2phen ligand.) It is important to note that the optical properties of the monoclinic phase are the same irrespective of whether the sample was obtained directly from the original preparation or from the maintenance of an orthorhombic crystal for several minutes at 150 °C, i.e., about 10 °C above the transition temperature.

In Figure 5 spectra of $Zn(4\text{-}ClPhS)_2(2,9\text{-}Me_2phen)$ are displayed. The emission from the low-temperature phase maximizes at 590 nm and that of the second phase at 550 nm. The latter emission is brighter (3×) than the former and can be generated either by holding the low-temperature phase at 193 °C for 3 min before mounting the crystals for study or using the translucent crystals that were originally separated mechanically from the mother liquor.

In Figure 6 the emission data for $Zn(PhS)_2(2,9\text{-}Me_2\text{-}4,7\text{-}Ph_2phen)$ are shown. When this compound is heated, the structured emission of the first phase is replaced by a diffuse band that is considerably *red-shifted* from the former and peaks at 650 nm. The latter spectrum was obtained by maintaining the originally obtained crystals at 132 °C for 3 min. This temperature is above the phase transition temperature but well below the melting point of the substance.

Although the decay times of the emissions are often nonexponential (see Table V), it is significant that they, too, are independent of the way the phase was produced. Decay curves from crystals of a high-temperature phase obtained directly upon crystallization are identical to those obtained from this same phase when it was generated by annealing the other phase, as previously described.

Discussion

The discovery of multiple crystalline phases of members of this class of complexes and the subsequent determinations of the two crystal structures of $Zn(PhS)_2(2,9\text{-}Me_2phen)$ are significant advances in our goal to understand the factors determining energy conversions among states in these substances. In particular, the origin of the previously reported thermal barriers to energy migration between $\pi\pi^*$ and ligand-ligand charge-transfer (LLCT) states is a major goal.[1] As the spectra clearly reveal, the dependence of the emission parameters on solid state structure is significant (vide infra). Although changes in lifetime are certainly expected since decay times are generally observed to be very sensitive to small perturbations of the structure, the large shifts in the emission energies were unexpected. Blue shifts of 2500 and 1200 cm^{-1} of peak maxima in the cases of $Zn(PhS)_2(2,9\text{-}Me_2phen)$ and $Zn(4\text{-}ClPhS)_2(2,9\text{-}Me_2phen)$, respectively, indicate major perturbations of the energy levels of the molecules subsequent to a thermally induced phase change.

Some correlations among the various sets of data are obvious. In general, at 77 K the low-temperature phases display shorter, often nonexponential, decay times and the spectra are much weaker than those from the high-temperature phases, which also yield decays at 77 K that are more nearly exponential (see Table V). In general, the emission band of the high-temperature phase is blue-shifted from that emanating from the other phase, but the $Zn(PhS)_2(2,9\text{-}Me_2\text{-}4,7\text{-}Ph_2phen)$ complex supplies the counter example. There appears to be a correlation between the ease of producing both crystalline forms simultaneously during preparation or recrystallization—the closer the phase-transition temperature is to the melting point, the better the chances for harvesting both types of crystals. This seems kinetically and thermodynamically reasonable. There may also be *more than one* low-temperature phase in some cases.

To search for structural factor(s) dictating the large energy shifts of the emissions between the two observed phases, we appeal to the detailed crystallographic data on $Zn(PhS)_2(2,9\text{-}Me_2phen)$. As Tables II and III show, only minor changes in bond lengths and angles occur when the crystallographic morphology changes. Moreover, both forms of the complex exhibit a pseudodimeric packing in the crystals, but the ring overlap with adjacent molecules is not especially extensive. Thus, we find no compelling reason to attribute the large spectral shift of the emission to *inter*molecular factors. Indeed, the only salient structural difference between the two forms appears to be the relative orientation of the thiol rings coordinated to the same zinc ion. In the monoclinic (high-temperature) phase the rings approach a face-to-face orientation and are, in fact, related by symmetry, but in the orthorhombic phase the two ring planes are almost perpendicular. The color of the crystal correlates with the emission; the deeper yellow crystal emits at longer wavelengths.

If one accepts the notion that the energy shift of the emission can be ascribed to the change in the orientation of the thiol rings, then the orbital natures of the excited states from which emission occurs must be considered. Previously the broad, diffuse bands from these complexes have been assigned to LLCT transitions.[6,7] Excitation of the complex to this kind of configuration transfers negative charge from the HOMO on the thiols to the LUMO on

(5) Wacholtz, W. F.; Jordan, K. J.; Crosby, G. A. Submitted for publication.

(6) Koester, V. J. *Chem. Phys. Lett.* **1975**, *32*, 575.

(7) Crosby, G. A.; Highland, R. G.; Truesdell, K. A. *Coord. Chem. Rev.* **1985**, *64*, 41.

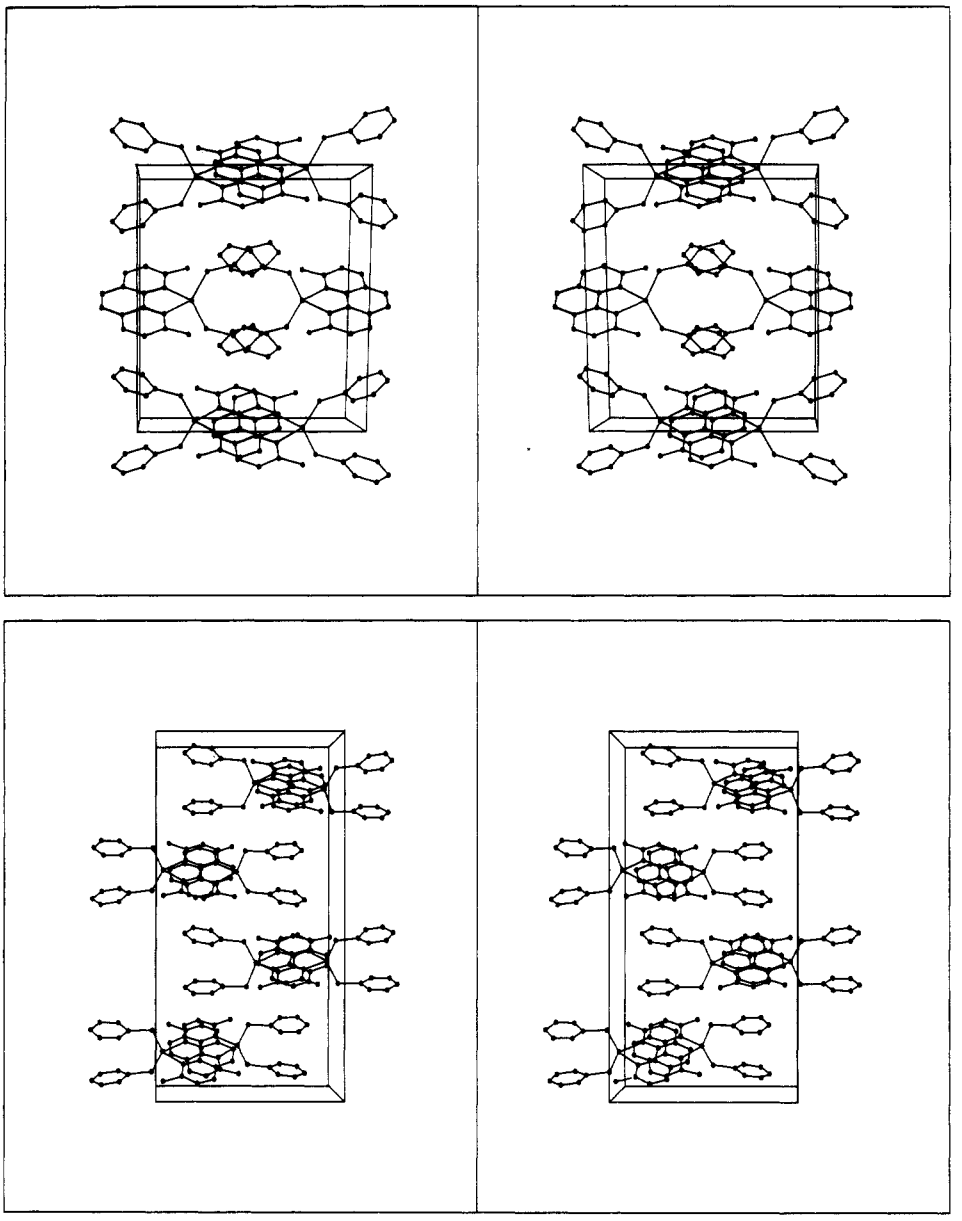

Figure 3. Stereopacking diagrams of $Zn(PhS)_2(2,9\text{-}Me_2phen)$: (top) monoclinic phase; (bottom) orthorhombic phase.

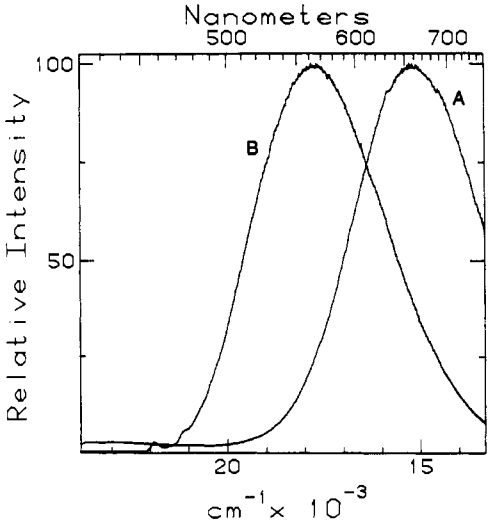

Figure 4. Normalized emission spectra of $Zn(PhS)_2(2,9\text{-}Me_2phen)$ at 77 K: (A) orthorhombic phase; (B) orthorhombic crystal after undergoing a phase transition. The B spectrum is identical with that obtained from crystals of the monoclinic phase. The B spectrum is much more intense (~5×) than the A spectrum.

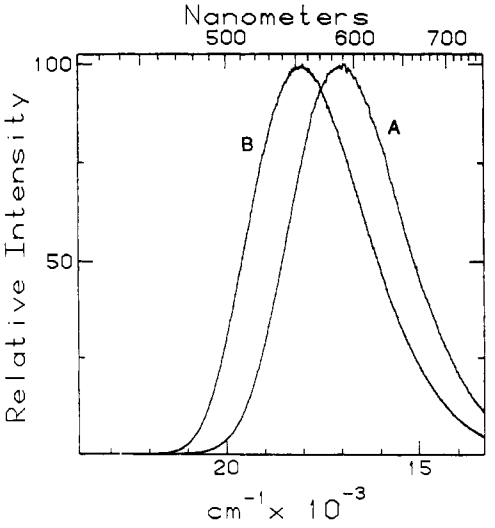

Figure 5. Normalized emission spectra of $Zn(4\text{-}ClPhS)_2(2,9\text{-}Me_2phen)$ at 77 K: (A) clear yellow crystals; (B) clear yellow crystals after undergoing a phase transition by heating. The B spectrum is identical to that obtained from the translucent yellow crystals originally harvested. The B system is more intense (~3×) than the A system.

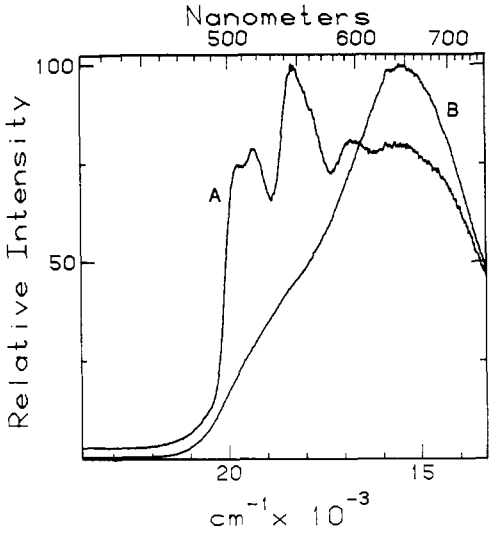

Figure 6. Normalized emission spectra of $Zn(PhS)_2(2,9\text{-}Me_2\text{-}4,7\text{-}Ph_2phen)$ at 77 K: (A) original crystals; (B) crystals after annealing at 132 °C (3 min).

the phenanthroline ligand. Face-to-face orientation of the thiol rings should lower the ground state and therefore raise the energy of the transition, precisely what is observed. This argument ignores the energy involved in twisting the plane of the one thiol ring with respect to the plane defined by the S, Zn, and S-linked carbon atom of the thiol ring. For aromatic thiols in the gas phase, this energy has been determined to be ca. 300 cm^{-1},[8,9] but the difference in twisting energy between a H–S and Zn–S linkage and the phenyl ring is unknown. If the ground-state energy of the twisted ring conformation is *raised* with respect to the face-to-face arrangement, as the gas-phase measurements on the ligand imply, then the emission from this form should also be red-shifted, as observed. Thus, we tentatively ascribe the observed blue shift of the emission spectrum of $Zn(PhS)_2(2,9\text{-}Me_2phen)$ to a stabilization of the ground electronic state of the complex due to the dispersion forces between the two face-to-face thiol rings and a possible barrier to twisting the thiol ring with respect to the plane of the Zn–S–C linkage. For the complex that displays a red shift of the emission when it is converted to the high-temperature form, one would predict a *destabilization* of the ground state in the latter phase. The relative thermodynamic stabilities of the phases would be governed by both energetic and entropic terms, however.

The results from these studies shed light on several problems we have encountered during our investigations of these and analogous closed-shell complexes. In glass matrices, we have never been able to obtain strictly exponential decays, and we are convinced that multiple conformations of the complexes lie at the root of the problem. Evidently, the lack of any strong electronic factors dictating the geometry allows several conformations of comparable energy to be realized in a glass matrix and produces both multiple decays and very broad LLCT bands.

For crystals, exponential decays are sometimes obtained at 77 K (Table V), but often the lifetimes are not strictly exponential. Moreover, in some cases, we have observed the decay of the same sample to change perceptibly with time (months). We attribute these changes to slow interconversion among phases. There is always the possibility of trap formation in the crystal and the possibility that traps are governing the luminescence. There is no doubt that the gross features (energy, band structure, and peak position) are determined by the molecular structure of a particular complex, since similar emission properties are observable when the substances are dissolved in plastics and glasses. The finer details, such as the nonexponentiality of some of the decays, could be controlled by traps, however, and measurements are in progress to shed light on this aspect of the problem.

The current results explain why thermally accessible barriers between $\pi\pi^*$ and LLCT excited states are difficult to design into the complexes by making subtle chemical substitutions on the chelated rings. Barriers only appear when the states separating them are nearly isoenergetic, i.e., lie within a few hundred wavenumbers.[10] Since conformational changes in the crystal lead to energy shifts that exceed this limit, then the somewhat capricious occurrence of thermally accessible barriers becomes understandable.

Finally, we comment on the relevance of these results to the fundamental process of charge separation in molecules and solids. If thermally surmounting barriers between $\pi\pi^*$ and LLCT excited states in these compounds do indeed represent irreversible conversion to a charge-separated configuration, then the sensitive dependence of the barrier height and, thereby, the rate of the charge separation process on the conformation of the complex could explain how very minor changes in structure can lead to enormous changes in charge separation (electron-transfer) rates in complex chemical systems.

Acknowledgment. This research was supported in part by the Office of Naval Research and the Department of Energy under Grant No. DE-FG06-87ER13809.

Registry No. $Zn(PhS)_2(2,9\text{-}Me_2phen)$, 117256-26-5; $Zn(4\text{-}ClPhS)_2(2,9\text{-}Me_2phen)$, 136301-32-1; $Zn(PhS)_2(2,9\text{-}Me_2\text{-}4,7\text{-}Ph_2phen)$, 136301-33-2.

Supplementary Material Available: Tables of X-ray data collection parameters (Table S1), bond lengths for the monoclinic and orthorhombic forms (Table S2), bond angles for the monoclinic and orthorhombic forms (Table S3), anisotropic thermal parameters for the monoclinic and orthorhombic forms (Table S4), and hydrogen atom positions and isotropic thermal parameters for the monoclinic and orthorhombic forms (Table S5) and stereopacking diagrams of bis(benzenethiolato)(2,9-dimethyl-1,10-phenanthroline)zinc(II) (Figure S1) (6 pages). Ordering information is given on any current masthead page.

(8) Schaefer, T.; Parr, W. J. E. *Can. J. Chem.* **1977**, *55*, 552.
(9) Larsen, N. W.; Nicolaisen, F. M. *J. Mol. Struct.* **1974**, *22*, 29.
(10) Van Houten, J.; Watts, R. J. *J. Am. Chem. Soc.* **1976**, *98*, 4853.